The Use of Impact Force as a Scale Parameter for the Impact Response of Composite Laminates

Wade C. Jackson
US Army Aerostructures Directorate, USAARTA-AVSCOM
Hampton, Virginia

C.C. Poe, Jr.
NASA Langley Research Center
Hampton, Virginia

Abstract

The building block approach is currently used to design composite structures. With this approach, the data from coupon tests are scaled up to determine the design of a structure. Current standard impact tests and methods of relating test data to other structures are not generally understood and are often used improperly. A methodology is outlined for using impact force as a scale parameter for delamination damage for impacts of simple plates. Dynamic analyses were used to define ranges of plate parameters and impact parameters where quasi-static analyses are valid. These ranges include most low-velocity impacts where the mass of the impacter is large and the size of the specimen is small. For large-mass impacts of moderately thick (0.35-0.70 cm) laminates, the maximum extent of delamination damage increased with increasing impact force and decreasing specimen thickness. For large-mass impact tests at a given kinetic energy, impact force and hence delamination size depends on specimen size, specimen thickness, boundary conditions, and indenter size and shape. If damage is reported in terms of impact force instead of kinetic energy, large-mass test results can be applied directly to other plates of the same thickness.

Symbols

d_o	diameter of damage
E_2	modulus transverse to the fiber direction
E_s	modulus of the impacter
F	contact force
F_i	contact force at initial load drop
F_{max}	maximum contact force
G_{II}	strain energy release rate for delamination growth due to interlaminar shear

S^*	critical value of the average transverse shear stress to extend a delamination (V^*/h)
h	thickness of plate
k	equivalent spring constant at center of plate
M	mass of impacter
n	Hertzian contact stiffness
r	radial distance from center of plate
r_c	radius of contact
r_i	radius of indenter
v	velocity of impacter
V	transverse shear force per unit length
V^*	transverse shear force associated with the delamination front
α	indentation
δ	displacement at center of plate
ν_s	Poisson's ratio of impacter

Introduction

Composite structures are currently designed and certified by a building block approach. First, critical areas of the structure are determined, and potential failure modes are identified. Then, a series of specimens is tested that will fail in modes that represent the failure modes in critical areas. The series begins with tests of simple coupons and ends with a test on a full-scale component. In between the coupons and full-scale component, tests are conducted on specimens containing joints and other types of details, subcomponents, and components. For composites, failure modes include interlaminar failure due to both in- and out-of-plane loads. Some of the more common failure sites are at open and loaded holes, impact locations, and hard points where stiffness changes dramatically. Environmental conditions are simulated for all but the full-scale tests. Even the full-scale test specimen may have to be environmentally conditioned if changes in environment cause changes in failure mode. This experimental process has produced reliable composite structures but is very expensive and contributes significantly to the cost of composite structures. In order to reduce costs, analytical methods are needed to bridge the gap between tests of simple coupons and verification tests of full-scale structures.

One of the more important failure modes in laminated composite materials involves nonvisible impact damage. Low-velocity (large-mass) impacts can cause nonvisible impact

damage that results in significant loss of strength [1-3]. The Federal Aviation Administration (FAA) requires that a structure with nonvisible impact damage carries an ultimate load. The purpose of the present paper is to show how impact force can be used as a scale parameter for delamination damage for impacts of simple plates. The use of kinetic energy as a scale parameter is also examined. By using a scale parameter in the building block approach to design for impact damage, the number of tests can be reduced, and the reliability can be improved. The parameters considered are plate size, boundary conditions, laminate thickness, material, visibility of damage, and type of damage. The impacter parameters considered are indenter diameter, mass, and velocity.

The damage resulting from an impact is considered in this paper but not the residual strength. If plate boundaries and structural elements are sufficiently remote from the impact damage, it is assumed that strength can be characterized solely by the damage state for a failure originating at the impact damage. Thus, identical damage is sufficient for identical strength. It is recognized that splices, stringers, and other structural elements are capable of arresting fractures resulting in greater strength than that of simple plates. In those cases, simple plate results are conservative.

Impact Analysis Models

Three analytical methods were used to predict the impact response of rectangular plates with fixed or simply-supported boundaries and with uniform thickness and density. With two of the methods, the response was predicted by solving elasto-dynamic plate equations. The third method predicted the maximum contact force and deflection during an impact by balancing the kinetic energy of the impacter with the work performed on the plate by the impacter. For all three methods, the impacter was assumed to be spherical and rigid, and indentation was calculated assuming Hertzian contact.

A dynamic method developed by Sankar [4] predicted the impact response by the use of a dynamic Green's function. With this approach, the nonlinear contact problem was uncoupled from the linear behavior of the plate. The contact problem was modeled with Hertz's law, and the plate response was predicted by the use of plate theory with shear deformation. This particular analysis program was limited to the analysis of a rectangular plate with simply-supported boundary conditions. The other dynamic method used a finite element plate code developed by Chen and Sun [5]. This analysis program also used Hertzian contact and included the effect of shear deformation. A uniform mesh with four-noded quadrilateral elements was used to model the plate for this study. All types of boundary conditions could be modelled using the finite elements. This analysis was also used to predict the static solution. The force histories from each of the two analyses were compared for the simply-supported case and were found to be nearly identical. The analysis using the dynamic Green's function was more efficient since many solutions could be quickly obtained from the generation of a single dynamic Green's function. Thus, the impact force was calculated using the dynamic Green's function program when the boundaries were simply supported and with the finite element program when the boundaries were clamped. The finite element program was also used to calculate the transverse shear force for all boundary conditions analyzed, even for simply-supported boundaries.

In reference 6, the maximum contact force and displacement were predicted using an equation obtained from an energy balance. This technique offered a simple method to quickly obtain the impact force as well as the peak impacter and plate displacements. The basic assumption for this analysis is that all the impacter's kinetic energy is transferred into the plate at the time of maximum contact force or maximum transverse deflection of the plate. Thus, peak contact force and peak plate displacement are assumed to occur as the impacter's velocity passes through

zero. Energy losses such as material damping and vibrations are neglected. With these assumptions, the energy balance can be written as

$$\frac{1}{2}Mv^2 = \int_0^{\delta_{max}} F\,d\delta + \int_0^{\alpha_{max}} F\,d\alpha \qquad (1)$$

where M and v are the mass and velocity of the impacter and δ and α represent the plate center displacement and contact indentation, respectively. The center deflection of the plate, δ, can be related to the contact force, F, by the linear equation

$$F = k\delta. \qquad (2)$$

where k is an equivalent spring constant for the plate. The spring constant can be easily calculated using plate theory or a single finite element run for more complicated boundary conditions. Since k is determined from a static analysis, the plate is assumed to deform in a static mode shape. Similarly, the contact indentation, α, is related to the contact force by Hertz's Law [6,7]

$$F = n\alpha^{3/2} \qquad (3)$$

where n is the Hertzian contact stiffness which can be approximated by the expression

$$n \approx \frac{4}{3} r_i^{1/2} E_2 \qquad (4)$$

where r_i is the radius of the indenter and E_2 is the modulus transverse to the fiber direction. By substituting (2) and (3) into (1) and integrating, the energy balance equation can be rewritten as

$$\frac{1}{2}Mv^2 = \frac{1}{2}\frac{F_{max}^2}{k} + \frac{2}{5}\frac{F_{max}^{5/3}}{n^{2/3}} \qquad (5)$$

Furthermore, the indentation and plate center deflection can be calculated through the use of (2) and (3) once F_{max} is known.

Force-Displacement Behavior During Impact

Instrumented impacters in falling-weight and pendulum impact tests can be used to record the contact force history. The force-displacement behavior can then be obtained by integration. Using this technique, numerous investigators have reported the contact force history and the force-displacement behavior for the impact of a composite plate [1,8-11]. A schematic of a typical force-time and force-displacement plot for a quasi-isotropic laminate with a brittle matrix is shown in Figure 1. As the impacter comes in contact with the plate, the contact force increases in a sinusoidal like manner with time and linearly with the displacement at the plate center. During quasi-static indentation tests, which have similar force-displacement plots, a crackling noise can often be heard during this phase of loading. The quasi-static indentation tests, however, do not have the small amplitude oscillations due to vibrations. Ultrasonic and microscopic inspections have revealed that matrix cracking and a small amount of delamination growth have occurred. As the force increases and a load, F_1, is reached, the force drops sharply indicating a sudden decrease in the transverse stiffness of the plate . This stiffness loss may be the result of large delamination growth. After the load drop, the contact force will increase further if the impacter has enough kinetic energy. A linear force-displacement behavior again develops where the slope after the load drop is less than the

slope prior to reaching F_I. Kwon and Sankar [8] have suggested that this linear relationship is the result of stable delamination growth. After the impacter begins to rebound, the force decreases until contact is lost. If force prediction methods do not account for the effect of damage, the predicted F_{MAX} will exceed the actual F_{MAX}. Investigators have reported a failure load, F_I, which was independent of impacter mass and velocity and of varying plate size and boundary conditions [1,8-11].

Delamination Damage

Data from several studies [8,9,13] are analyzed to illustrate a method for predicting the maximum extent of delamination in moderately thick (0.34 - 0.70 cm) laminates. The diameter of the delaminated region, which was much larger than the contact region, was calculated in terms of the maximum contact force and the transverse shear force.

A study of impact damage in 0.70-cm-thick $[45/0/-45/90]_{6S}$ quasi-isotropic AS4/3501-6 and IM7/8551-7 composite laminates was conducted for static indentation and falling-weight impact tests [13]. The same indenter size (1.27-cm-diameter hemisphere) was used for all tests. The mass of the falling-weight impacter was 4.63 kg. The specimens in the static indentation tests were clamped over a 10.2-cm circular opening, whereas the specimens in the impact tests were clamped over a 12.7-cm square opening. The diameter of damage from C-scan images is plotted against impact force in Figures 2 and 3 for the AS4/3501-6 and IM7/8551-7 materials, respectively. The C-scan image depicts a cumulative planar measure of the extent of delamination. Open symbols indicate nonvisible surface damage, and filled symbols indicate visible surface damage. Initial damage was not evident on the surface. Cross-sections of some damaged specimens were examined, revealing that the damage in the contact area consisted of matrix cracks, delaminations, and broken fibers. The damage away from the contact area consisted of a combination of matrix cracks and delaminations which formed a spiral stair-case pattern involving 11 interfaces. This damage pattern was common to both the toughened (IM7/8551-7) and untoughened (AS4/3501-6) material systems. The maximum delamination diameter increased linearly with impact force for both material systems. The dashed lines represent a linear regression analysis through the origin. There was no significant difference in delamination diameter between the static and dynamic test methods for either material system.

Since there is a linear relationship between impact force and maximum delamination diameter, a constant value of transverse shear force can be associated with the delamination front. For circular isotropic plates, the shear force per unit length, V, is given by

$$V = \frac{F}{2\pi r} \tag{6}$$

where F is the impact or contact force and r is a radial distance which is much greater than the contact radius, r_c (i.e. $r >> r_c$). This shear force expression (6) is also valid for rectangular plates where r is much greater than r_c and much less than the plate dimensions. Assuming Hertzian contact [6], the contact radius, r_c, can be calculated using the expression

$$r_c = \left(\frac{F r_i^{3/2}}{n}\right)^{1/3} . \tag{7}$$

The transverse shear force, V^*, associated with the edge of the delamination can be calculated from the slope of the impact force - delamination diameter line by using the expression

$$V^* = \frac{F}{\pi d_0} \tag{8}$$

where $d_0 = 2r$ is the maximum delamination diameter. The value of V^* for each regression line is shown. For the AS4/3501-6 data in Figure 2, V^* equals 72.1 kN/m, and for the IM7/8551-7 data in Figure 3, V^* equals 158 kN/m. For both materials, the experimental data is in good agreement with equation (8) after the delaminations have initiated. The maximum delamination diameter for a given impact force was not affected by plate size, shape, or the method of impact. The value of V^* and the contact force for delamination initiation and penetration are greater for the IM7/8551-7 than those for the AS4/3501-6 laminates. Thus, the toughened material shows superior impact resistance.

A study of impact damage [9] was conducted using a smaller 7.62- x 7.62-cm frame and an instrumented falling-weight impacter (2.74 kg) with a 1.27-cm diameter indenter. The impact specimens were 24- and 48-ply quasi-isotropic $[-45/0/45/90]_{ns}$ laminates made of AS4/3501-6. The average thickness was 0.343 cm for the 24-ply laminates and 0.681 cm for 48-ply laminates. The results from that study are plotted in Figure 4 in the same manner as in the previous two figures. Again, a linear relationship existed between impact force and maximum delamination diameter for both the 24- and 48-ply laminates. The values of V^* computed by a linear regression for the 24- and 48-ply laminates were 40.7 and 80.2 kN/m, respectively. Also, for the 48-ply laminates, the values of V^* in Figures 2 and 4 were reasonably close (less than an 11% difference).

Another study of impact damage was reported in reference 8. In this study, both quasi-static indentation and instrumented pendulum impact tests were used. The impact specimens were 32-ply quasi-isotropic $[0/45/90/-45]_{4s}$ laminates of AS4/3501-6. The average thickness of the laminates was 0.454 cm. The specimens were simply-supported over rings with diameters of 5.08, 7.62, and 10.2 cm. Two steel hemispherical indenters were used with diameters of 0.635 and 2.54 cm. The delamination diameter from the C-scans is plotted against impact force in Figure 5. When all of the data points are plotted together, a linear relationship is found between impact force and delamination diameter. This suggests that delamination away from the contact area is only a function of impact force and not of support diameter, indenter diameter, or method of impact. A value of $V^* = 41.5$ kN/m was calculated using a linear regression. Equation (8) is in good agreement with the experimental data points.

The value of critical shear force, V^*, for each of the four experimental data sets is plotted against laminate thickness in Figure 6. Two curves are fitted through the data points corresponding to V^* being proportional to h or to $h^{3/2}$ where h is laminate thickness. If V^* is proportional to h, then the delamination front can be associated with a constant value of the average transverse shear stress, $S^* = V^*/h$. For the data in Figure 6, a value of 10.8 MPa was calculated for S^* using a linear regression. This value of S^* is not an interlaminar shear strength since extending the delamination involves a complex interaction with matrix cracks. Hence, the delamination front is not in a state of pure shear. Also, this value of S^* is an order of magnitude less than the transverse shear strength of 124 MPa reported in reference 13 for AS4/3501-6. If the delamination front can be associated with a constant value of shear stress, then a single value of S^* may be used over a range of thicknesses as long as the material and layup sequence are kept constant. The other curve, V^* proportional to $h^{3/2}$, corresponds to the relationship between delamination length and thickness for an end-notched flexure specimen with constant G_{II} and applied load [14]. The three-point loading of the end-notched flexure specimen involves flexure similar to the transverse loading of a plate. Both relationships are in reasonable agreement with the data. Data over a wider range of h are required to determine the exact relationship between V^* and h.

Dynamic Response

The Impact Force Curve

Using a dynamic analysis program, force histories were generated for the impact of a 12.7- x 12.7-cm rectangular simply-supported quasi-isotropic plate. A few force histories at a kinetic energy of 13.6 J are shown in Figure 7. For large-mass impacts such as the 4.63-kg impact, the histories were composed of many small oscillations superimposed on the forced response. These oscillations in the force are due to the plate vibrating against the impacter during contact. For small-mass impacts such as the 0.025-kg impact, the contact duration was much shorter and the oscillations did not have time to develop. This type of response is typical of an impact from a fired projectile for a gas-gun impact test. For an impact with a mass of 0.30 kg, the force history was dominated by several large oscillations superimposed on the forced response.

A series of solutions was generated where the plate parameters were held constant, and the impacter mass and velocity were varied such that the kinetic energy remained constant. The peak contact force (referred to as impact force) from each of these runs was then plotted against the reciprocal of the impacter mass, M^{-1}, on a logarithmic scale for a given value of kinetic energy. The impact force curves at three kinetic energies for the impact of a 12.7- x 12.7-cm plate with simply-supported boundaries are shown in Figure 8. Moving to the right on a curve of constant kinetic energy corresponds to decreasing mass and increasing velocity. Approximately 20 runs were necessary to establish each impact force curve.

On the left side of the curve (large mass - low velocity), the contact duration is much longer than the time required for flexural waves to be reflected from the boundaries. It is the continual propagation and reflection of waves in the bounded plate that brings about a state of static equilibrium. During the long contact period, the flexural waves have time to propagate and reflect many times which results in a deformation mode approaching the static solution. Impact force predictions from an energy-balance analysis (eq. (4) - dashed lines) are also plotted for each kinetic energy on the figure for comparison. For large masses, the impact force approached the value predicted by the energy-balance analysis indicating a static deformation mode. In this region, the impact force is relatively constant over a range of masses and velocities at a given kinetic energy. On the right side of the curve (small mass - high velocity), the contact duration is very short. No oscillations occurred in the force history since there was insufficient time for flexural waves to reflect from the boundaries. The impact force was not independent of mass and velocity for a given kinetic energy in this region. A transitional region exists between the large-mass and small-mass region which is characterized by a force history that is dominated by a few large amplitude oscillations. Multiple contacts may also occur in this region. The impact force curve was divided into three regions (Figure 8) according to impact mechanics: static (large mass), transitional, and dynamic (small mass). These three regions are represented by the curves shown in Figure 7. For higher kinetic energies in Figure 8, the impact force curves shifted vertically, maintaining the same approximate structure. For large-mass impacts, the energy-balance analysis accurately predicted the increase of impact force with kinetic energy.

The variation of the impact force curve with changing boundary conditions and plate size is shown in Figure 9. Impact force curves for two small 12.7- x 12.7-cm plates with different boundary conditions (simply-supported and clamped) are shown. Also shown is the impact force curve for a larger 25.4- x 25.4-cm plate with simply-supported boundaries. For large-mass impacts (left side of curve), the impact force was larger for clamped boundaries than for simply-supported boundaries due to the increased transverse stiffness. Similarly, when the plate size was doubled, the impact force was less for the large-mass impact due to the decreased transverse stiffness. Also, a larger mass is required for the larger plate to deform in a static manner. This is indicated by the larger difference between the impact force for the energy-balance solution

and the impact force curve at very large masses. Quasi-static response only occurs when the impacter's mass is large and the size of the target is relatively small. During the long contact period associated with large-mass impacts, the flexural waves have time to propagate and reflect many times which results in a deformation mode approaching the static solution. However, if the plate is large, the flexural waves take much longer to reflect from the boundaries, and the deformation mode diverges from the static mode. Consequently, the impacter mass must be extremely large to ensure a contact duration long enough for the waves to reflect many times for large plates. Therefore, a static deformation mode will not develop for the impact of large plates and structures except for very large mass impacters. This failure to respond quasi-statically was also observed for the impact of large rings by very large masses [3].

For small-mass (high-velocity) impacts, the three curves converged which indicates that the impact force is independent of boundary conditions and plate size. The small difference between the curves reflects the inaccuracies of the modeling and differences between the computer codes. The convergence of the curves is due to the fact that the flexural waves do not have time to reflect from the boundaries before the peak contact force occurs. Consequently, a specific impacter mass and velocity combination will result in the same impact force regardless of plate size or boundary conditions as long as the impact response is of the dynamic type. The large plate enters the dynamic response region the earliest since the flexural waves take the longest time to reflect from the boundaries.

Transverse Shear Force

The transverse shear force history during impact was calculated at a point 3.18 cm from the center of a 12.7- x 12.7-cm simply-supported plate. The 3.18-cm distance corresponds to the larger delamination diameters in Figures 2-5. It is also much greater than the contact diameter, eliminating the influence of the contact stresses. The finite element code was used to calculate the impact response for a range of impacter masses and velocities at two kinetic energies. The maximum shear force was normalized by the static shear force calculated for the peak contact force. This normalized shear force was then plotted against the log of the reciprocal of the impacter mass, $\log(M^{-1})$, to create curves for impacts of the same kinetic energy similar to the impact force curves. Figure 10 shows two shear force curves for impact energies of 13.6 and 20.3 J. Since the normalized shear force was greater than unity for all masses, the shear force increased at a faster rate than the impact force. The difference between the static and dynamic shear forces was greatest, in general, for the smaller masses. However, the shear force was within 10% of the static shear force up to $m^{-1} = 1.6\ kg^{-1}$ (masses greater than 0.63 kg). Consequently, a static analysis, such as equation (6), should be adequate to obtain the transverse shear force for impacts in the large-mass region. In the small-mass region, however, the plate stresses and deformations tend to reach maximum values after the contact period is over. At the maximum values, the plate stresses and deformations may even be in the opposite direction of those in the static case. This phenomenon is due to the complex nature of wave propagation and reflection. The treatment of these stresses is beyond the scope of this paper.

Similar curves of normalized shear force, at a point 3.175 cm from the plate center, versus M^{-1} are plotted in Figure 11 for the impact of a 12.7- x 12.7-cm clamped plate and for a larger 25.4- x 25.4-cm simply-supported plate. Again, the shear force for the smaller two plates was within 10% of the values predicted by a static analysis for impacts in the large-mass region. However, the dynamic shear force for the large plate was more than 25% greater than the predicted static value which indicates that the large plate is not deforming in a static manner.

Maximum Delamination Diameter

For 48-ply AS4/3501-6 plates, the diameter of delaminations was computed using an energy balance, equation (4), and the critical transverse shear force , equation (8). The results, which are applicable to large-mass impacts, are shown in Figure 12 for two values of kinetic energy, two plate sizes, two thicknesses, and for clamped and simply-supported edges. The quasi-isotropic plates were 24- or 48-plies thick, and the hemispherical indenter diameter was 1.27 cm. The critical values of the transverse shear force, V^*, were 40.7 and 72.1 kN/m for the 24- and 48-ply laminates, respectively. The predicted value of impact force is shown above each bar. For a given plate thickness, the maximum delamination diameter increased in proportion to impact force after delamination initiated. For a given value of kinetic energy, the impact force and hence maximum delamination diameter depend strongly on plate size, plate thickness, and boundary conditions for large-mass (low-velocity) impacts.

Design Allowables from Coupon Tests

Kinetic Energy as an Impact Parameter

For large impacter masses (low velocities) and a fixed value of kinetic energy, the analyses show that delamination damage does not vary with mass and velocity but does vary with transverse plate stiffness which is a function of plate size and boundary conditions. However, for maximum delamination diameter not to vary with mass and velocity for large plates, the mass must be much larger than for small plates. Thus, impact test results can be compared in terms of kinetic energy only when the impacter mass is large and the plates are small and have the same transverse stiffness. For small impacter masses (high velocities), on the other hand, the impact force and hence the stresses do vary with mass and velocity when kinetic energy is a constant. Therefore, kinetic energy cannot be used in general as a parameter to compare impact damage or to predict impact damage in structures from coupon tests.

Impact Force as an Impact Parameter

When impact force is a constant and impacter mass is large, the analyses show that the maximum delamination diameter does not vary with mass and velocity nor with plate size and boundary conditions. Therefore, impact force can be used as a parameter to compare impact damage or to predict impact damage in structures from coupon tests. However, the maximum extent of delaminations must be some minimum distance from the coupon boundary and from any hard point, reinforcement, or boundary of the structure. Impact forces are routinely measured in falling-weight tests using instrumented impacters and hence are available from experiments. Impact forces can also be predicted from kinetic energy for small plates using a static analysis with a simple energy balance equation. Of course, such predictions overestimate the actual impact force when significant damage develops.

For small impacter masses (high velocities), on the other hand, the transverse shear force does vary with mass and velocity when impact force is a constant, and impact force cannot be used as a parameter to compare impact damage or to predict impact damage in structures from coupon tests. Perhaps, only plate stresses can be used in this regime. At this time, no convenient methods for measuring impact force and transverse shear force have been reported for small impacter masses like those in gas gun tests. Such a capability would assist in verifying the analyses.

Nonvisible Damage as an Impact Parameter

As shown in the previous sections, the use of kinetic energy and impact force as impact parameters does have disadvantages. On the other hand, the use of a level of visible or nonvisible damage may eliminate the need for a dynamic analysis and the measurement of impact force or stresses. In this case, the residual strength could be determined for a certain level of visible or nonvisible damage, irrespective of kinetic energy or impact force. The maximum level of visible impact damage would be that level that is unlikely to be overlooked. Conversely, the minimum level of visible impact damage would be that level that is likely to be overlooked. Some metric for visibility like residual impression depth should be used to reduce subjectivity. For example, the United States Air Force currently defines visible damage as a 0.254-cm-deep dent [15], and Hercules demonstrated that 0.013-cm-deep depressions could be found reliably in a thick filament-wound rocket motor case [16]. Additional work needs to be done to determine the effect of impacter shape and laminate thickness on nonvisible damage.

Concluding Remarks

Dynamic analyses were made of simple plates to calculate time histories of contact force and transverse shear force. Impacter mass and velocity and plate configuration were varied. Experimental data for quasi-isotropic laminates 0.35- to 0.70-cm thick were analyzed to determine a method for predicting delamination damage size in terms of transverse shear force. The experimental data were from falling weight and pendulum impact tests and static indentation tests. The effects of impacter and plate parameters on maximum size of delamination damage were calculated using predicted values of transverse shear force.

For large-mass (low-velocity) impacts of a given kinetic energy, the dynamic analyses indicated that the impact force (peak contact force) decreases with increasing plate size and is smaller for simply-supported plates than clamped plates. Also, impact force can be predicted using simple energy-balance equations, and transverse shear force can be predicted using a static solution. However, the mass must increase with increasing plate size in order for this static representation to remain valid. The large-mass impact tests and static indentation tests indicate that delamination damage which corresponds to a constant value of transverse shear force, V^*, at the delamination front increased in proportion to impact force. The critical shear force, V^*, increased approximately in proportion to thickness. For a constant value of V^* and kinetic energy, the dynamic analyses indicate that the size of delamination damage will decrease with increasing plate size and will be smaller for simply-supported plates than clamped plates. However, for a given impact force, size of delamination damage will be independent of plate configuration. Therefore, for large-mass (low-velocity) impacts, only impact force can be used as a sole parameter to predict the maximum size of delamination damage in simple plates or structures from that in coupons.

For small mass (high-velocity) impact, the dynamic analyses indicate that impact force increases with decreasing mass for a given plate configuration and a given value of kinetic energy and that the transverse shear force cannot be represented by static values. Furthermore, the peak shear force may occur after contact and may even be of the opposite sense as that of the static solution. Therefore, for small mass (high-velocity) impacts, neither kinetic energy nor impact force can be used as a sole parameter to predict the size of delamination damage.

References

1. Byers, B. A.: Behavior of Damaged Graphite/Epoxy Laminates Under Compression Loading. NASA CR-159293, August 1980.

2. Rhodes, M. D.: Impact Tests on Fibrous Composite Sandwich Structures. NASA TM-78719, October 1978.

3. Poe, C. C., Jr.: Summary of a Study to Determine Low-Velocity Impact Damage and Residual Tension Strength for a Thick Graphite/Epoxy Motor Case. NASA TM-102678, June 1990.

4. Sankar, B. V.: A Modified Green's Function for Computing Structural Response due to Low-Velocity Impact. Technical Report No. AeMES-TR-1-36, Department of Aerospace Engineering, Mechanics & Engineering Science, University of Florida, October 1990.

5. Chen, J. K. and Sun, C. T.: Analysis of Impact Response of Initially Stressed and Buckled Composite Laminates. Tech. Report CML 84-6, Purdue University, April 1984.

6. Greszczuk, L. B.: Damage in Composite Materials Due to Low Velocity Impact. Impact Dynamics, edited by L. A. Zukas et al., John Wiley & Sons, New York, 1982, p. 55.

7. Sun, C. T.: An Analytical Method for Evaluation of Impact Damage Energy of Laminated Composites. Composite Materials: Testing and Design, ASTM STP 617, American Society for Testing Materials, 1977, pp. 427-440.

8. Kwon, Y. S. and Sankar, B. V.: Indentation-Flexure Damage in Graphite/Epoxy Laminates. NASA CR-187624, 1991.

9 Srinivasan, K., Jackson, W. C., and Hinkley, J. A.: Response of Composite Materials to Low Velocity Impact. NASA TM-102755, January 1991.

10. Sjöblom, P. O., Hartness, J. T., and Cordell, T. M.: On Low-Velocity Impact Testing of Composite Materials. Journal of Composite Materials, Vol. 22,. January 1988, pp. 30-52.

11. Sjöblom, P. O.: Simple Design Approach Against Low-Velocity Impact Damage. Proceedings of the 32nd International SAMPE Symposium, April 6-9, 1987, pp. 529-539.

12. Poe, C. C., Jr.; Portanova, M. A.; Masters, J. E.; Sankar, B. V.; and Jackson, W. C.: Comparison of Impact Results for Several Polymeric Composites over a Wide Range of Low Impact Velocities. NASA CP-3104, 1990.

13. Sun, C. T., and Kelly, S. R.: Failure in Composite Angle Structures, Part: I, Initial Failure. J. of Reinforced Plastics and Composites, Vol. 7, May 1988, pp. 220-232.

14. Russell, A. J.: On the Measurement of Mode II Interlaminar Fracture Energies. Defense Research Establishment Pacific (DREP), Victoria, British Columbia, Canada, Materials Report 82-0, Dec. 1982.

15. Lincoln, J.: Certification of Composites for Aircraft. NASA CP-10075, March 1991, pp. 401-420.

16. Madsen, C. B., Morgan, M. E., and Nuismer, R. J.: Impacting Large Composite Structures and Scaling Impact Response and Damage. NASA CP 10075, March 1991, pp. 27-78.

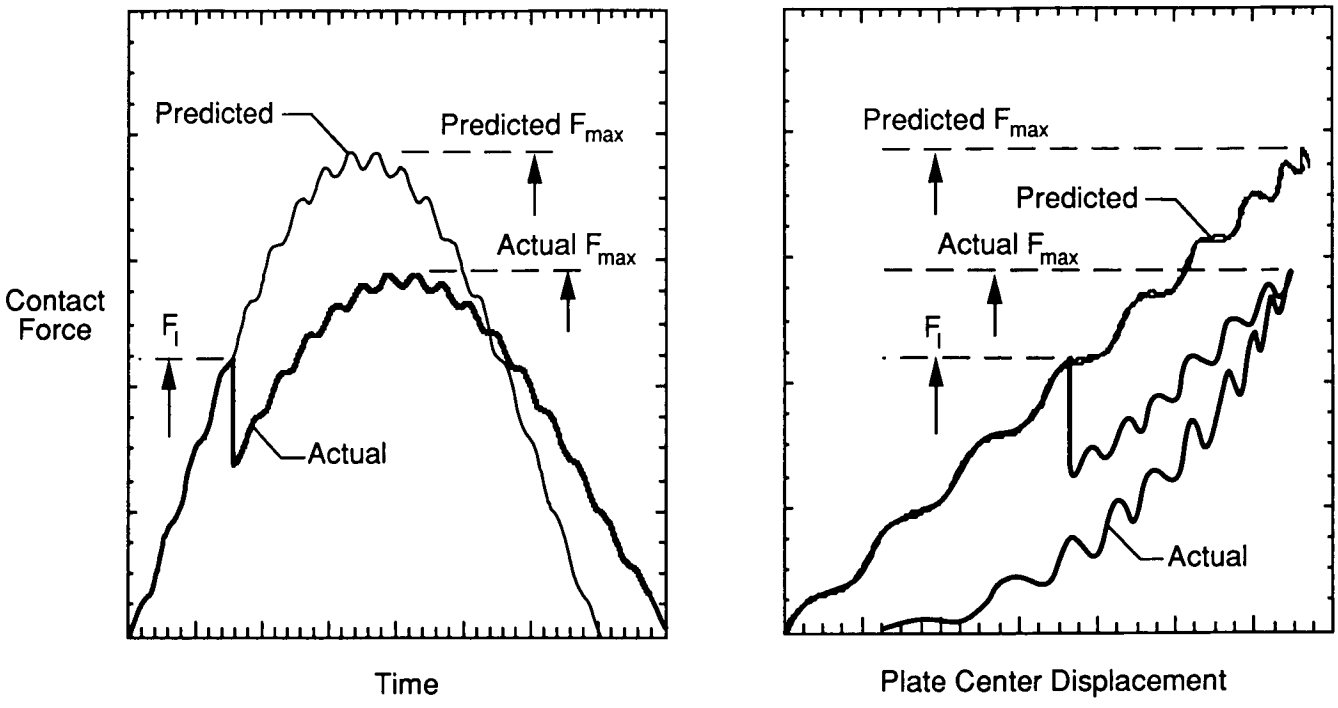

Figure 1. Schematic of a typical force-time and force-displacement plot.

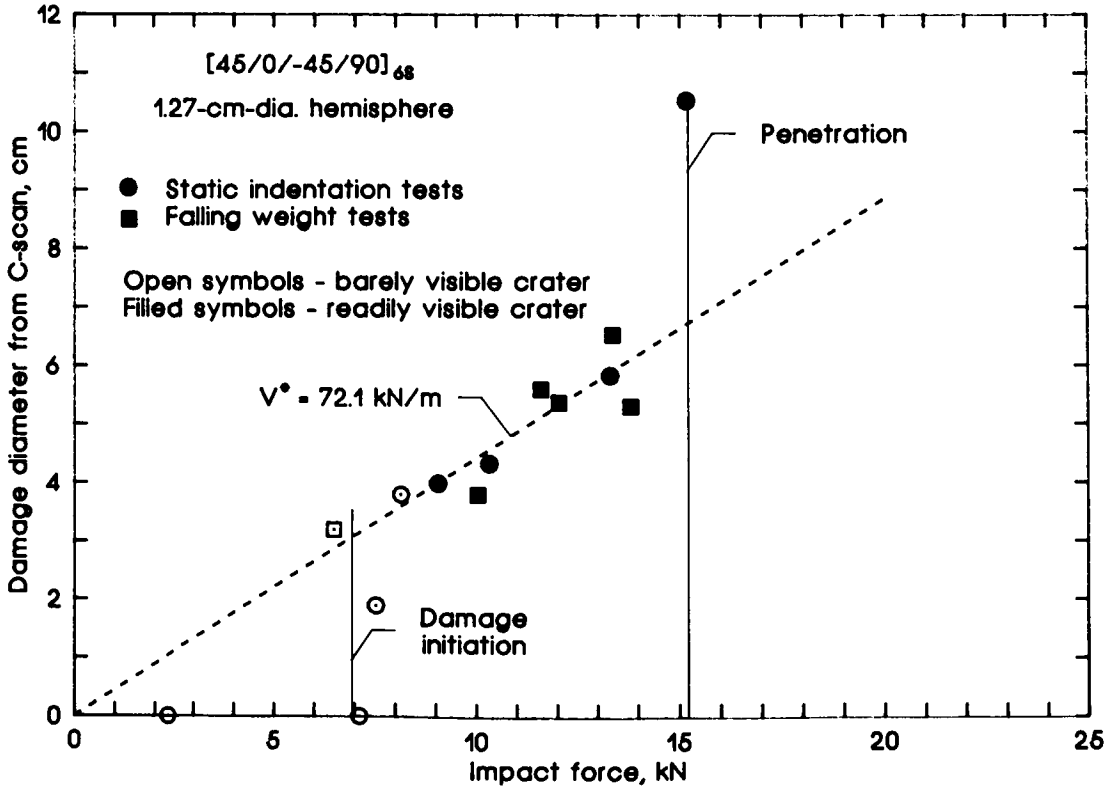

Figure 2.- Damage diameter versus impact force for 48-ply quasi-isotropic AS4/3501-6 laminates.

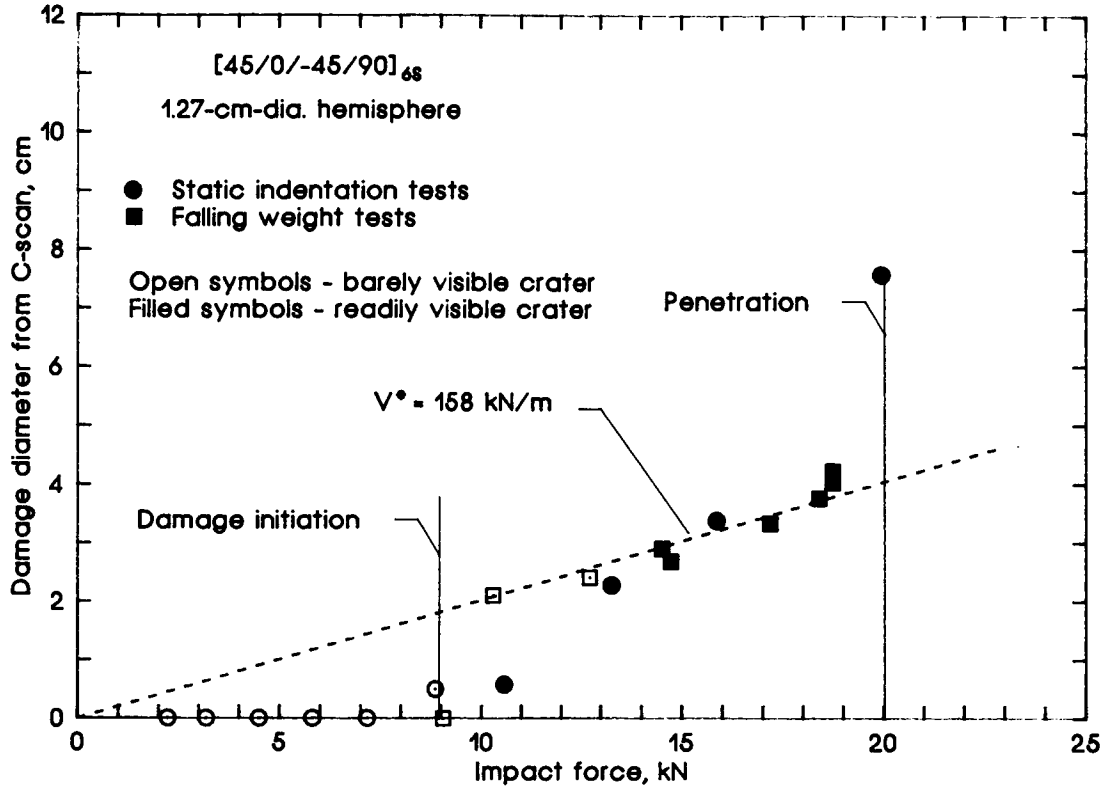

Figure 3.- Damage diameter versus impact force for 48-ply quasi-isotropic IM7/8551-7 laminates.

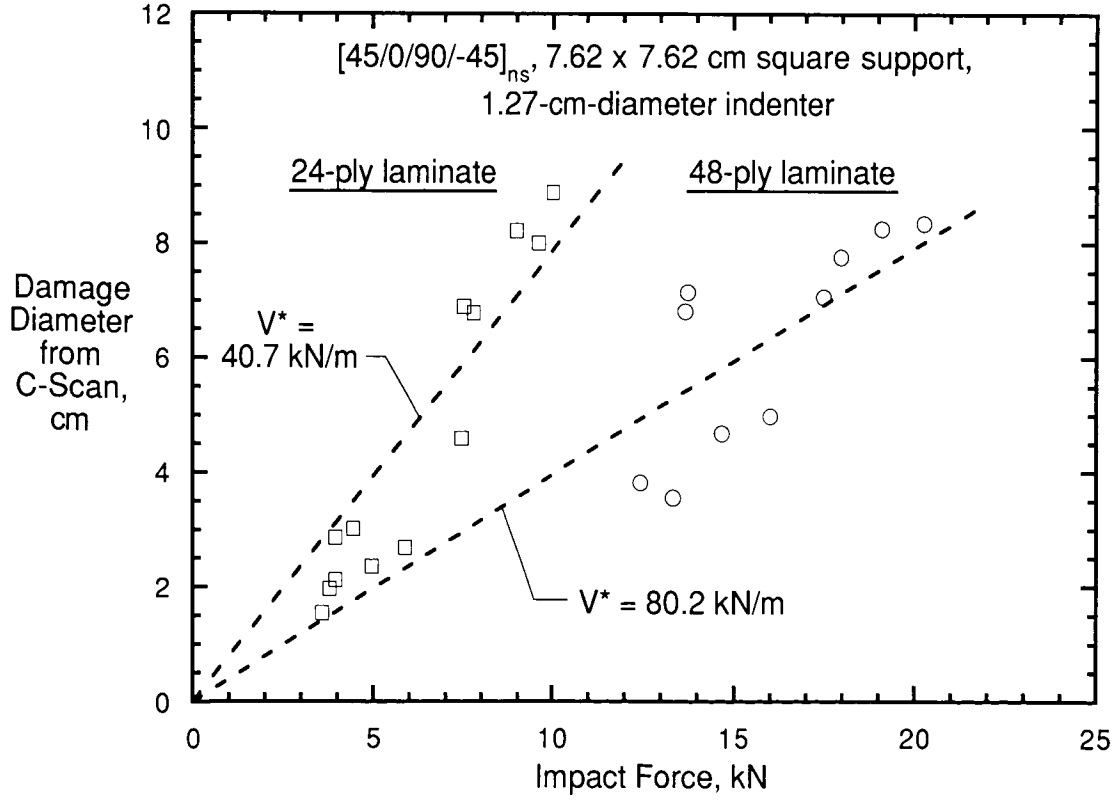

Figure 4. Delamination diameter versus impact force for 24- and 48-ply quasi-isotropic AS4/3501-6 laminates.

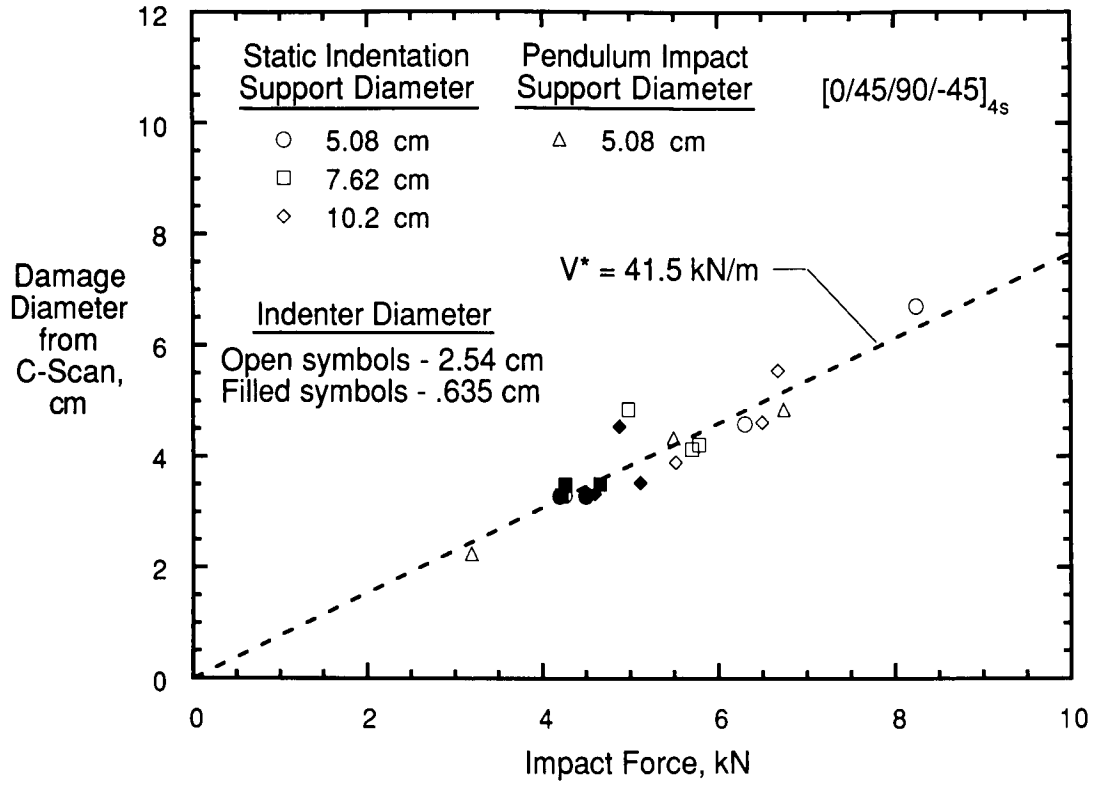

Figure 5. Delamination diameter versus impact force for 32-ply quasi-isotropic AS4/3501-6 laminates.

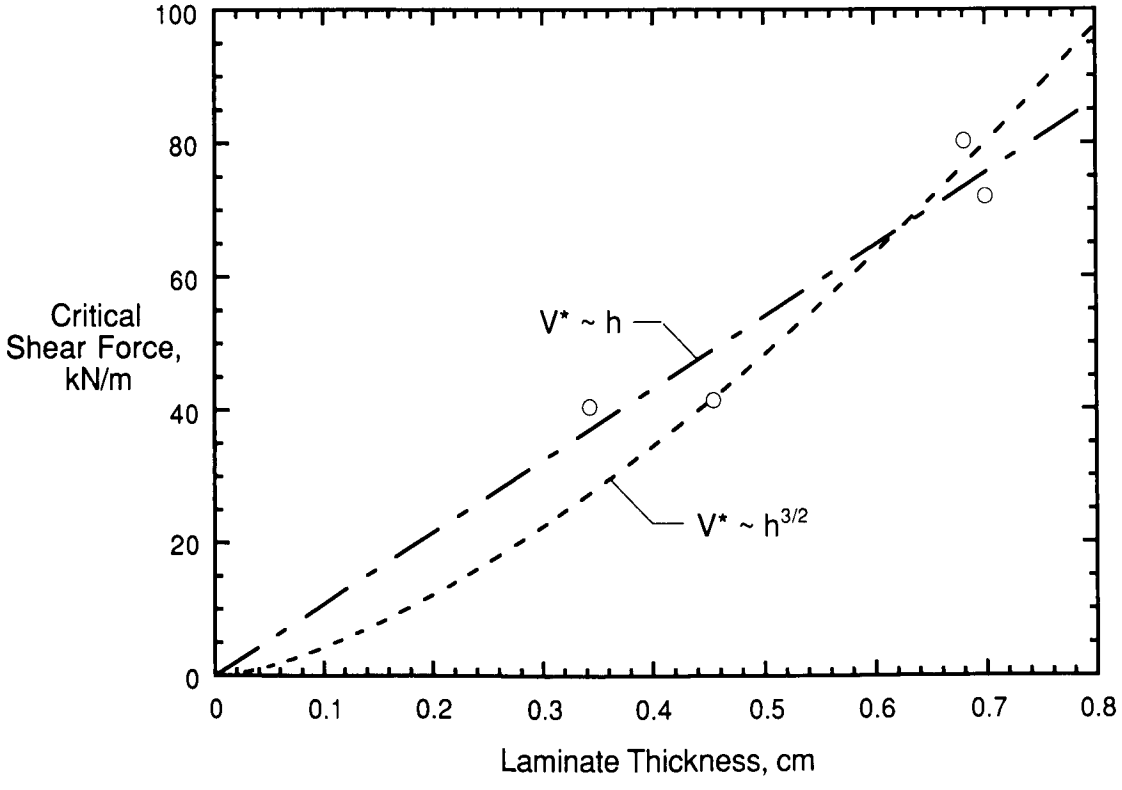

Figure 6. Effect of laminate thickness on the critical transverse shear force.

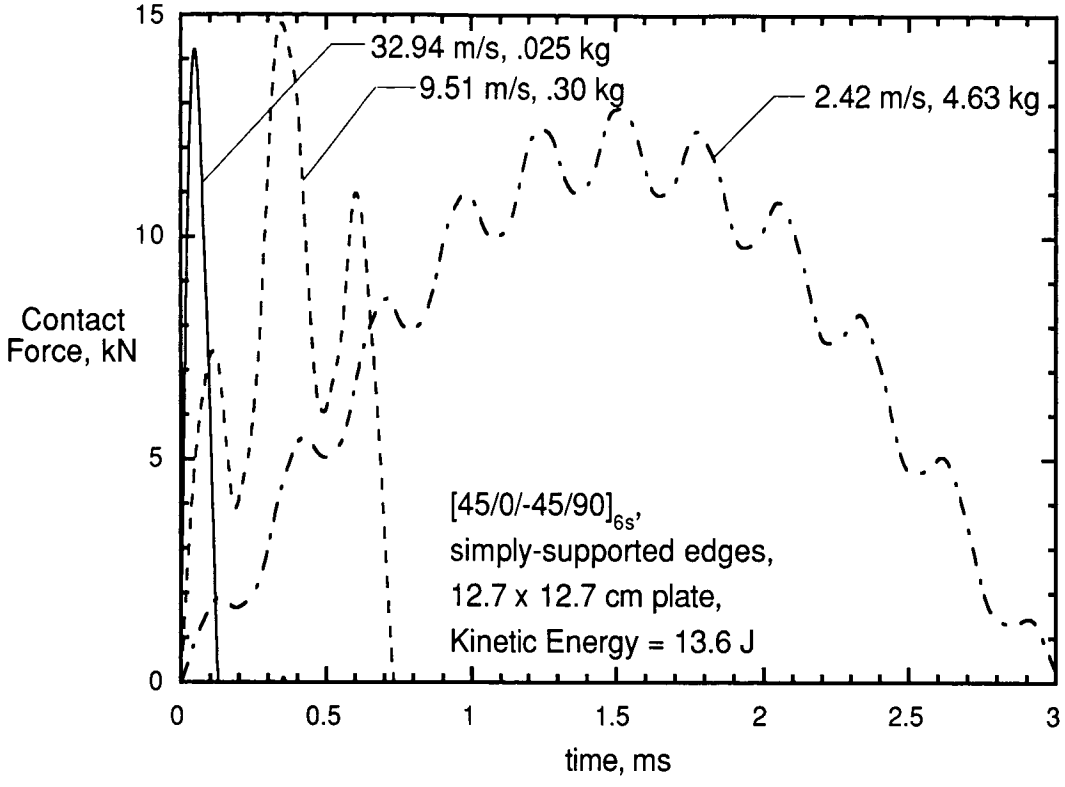

Figure 7. Predicted contact force history for several impacter mass and velocity combinations at 13.6 J.

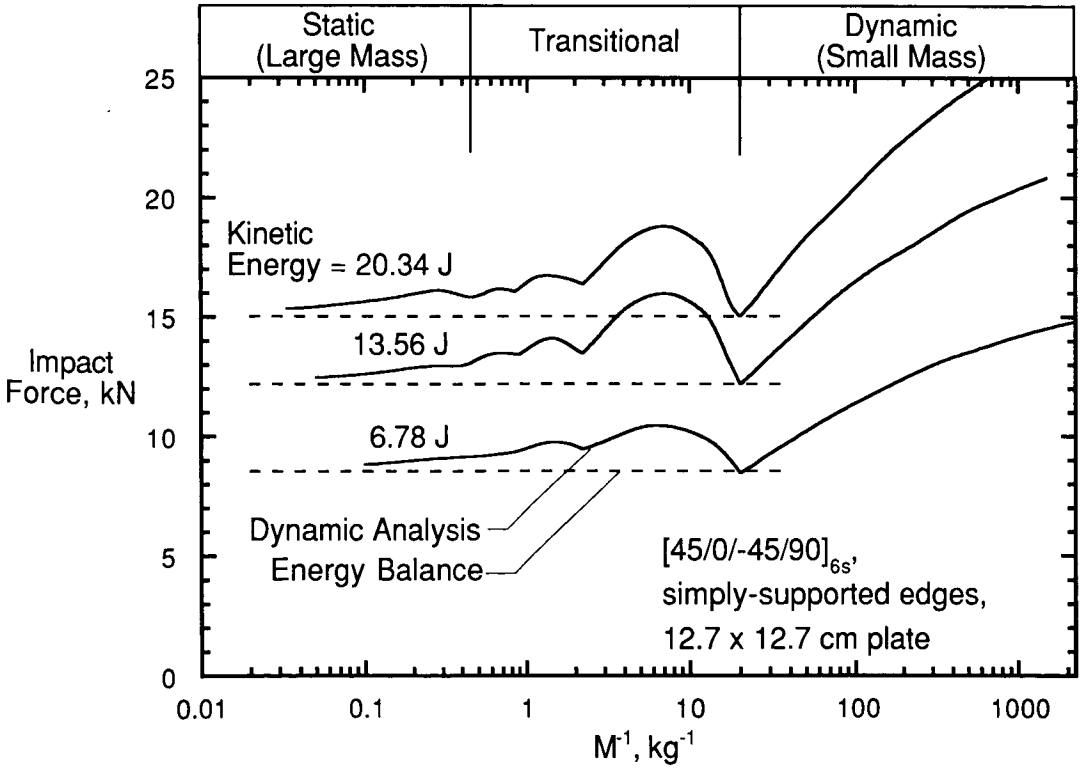

Figure 8. Predicted impact force versus impacter mass at constant kinetic energies.

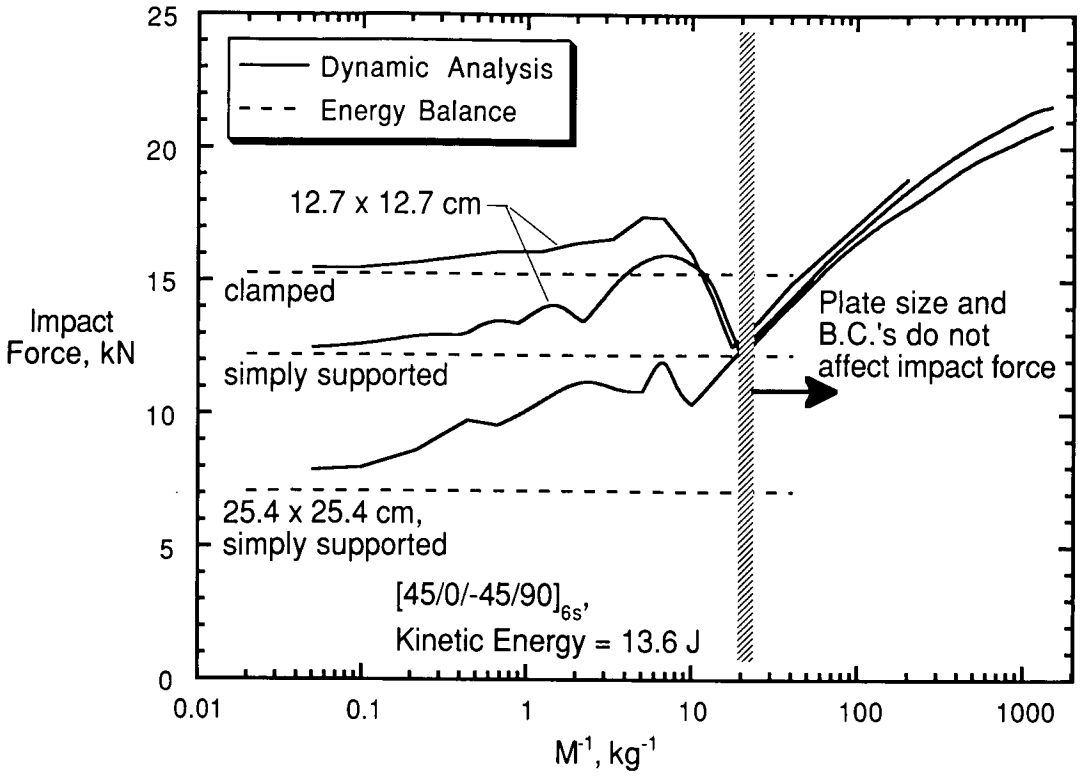

Figure 9. Impact force versus M^{-1} for various plate sizes and boundary conditions.

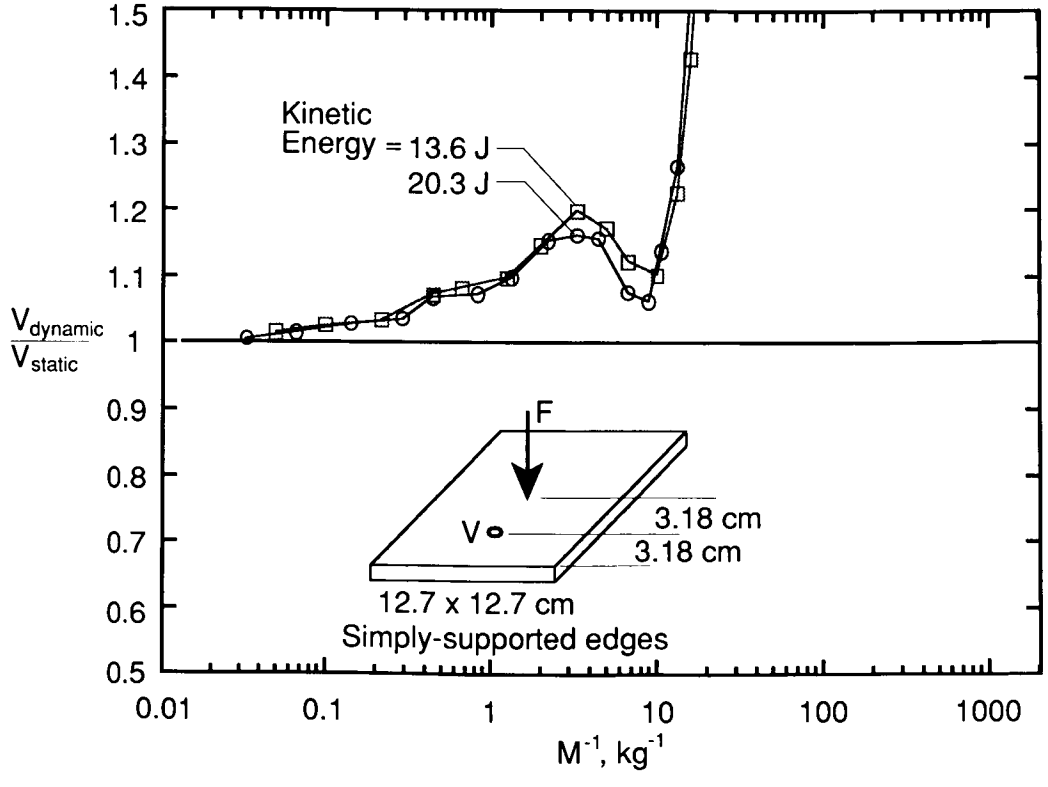

Figure 10. Normalized shear force versus M^{-1} for an impact with a kinetic energy of 13.6 and 20.3 J.

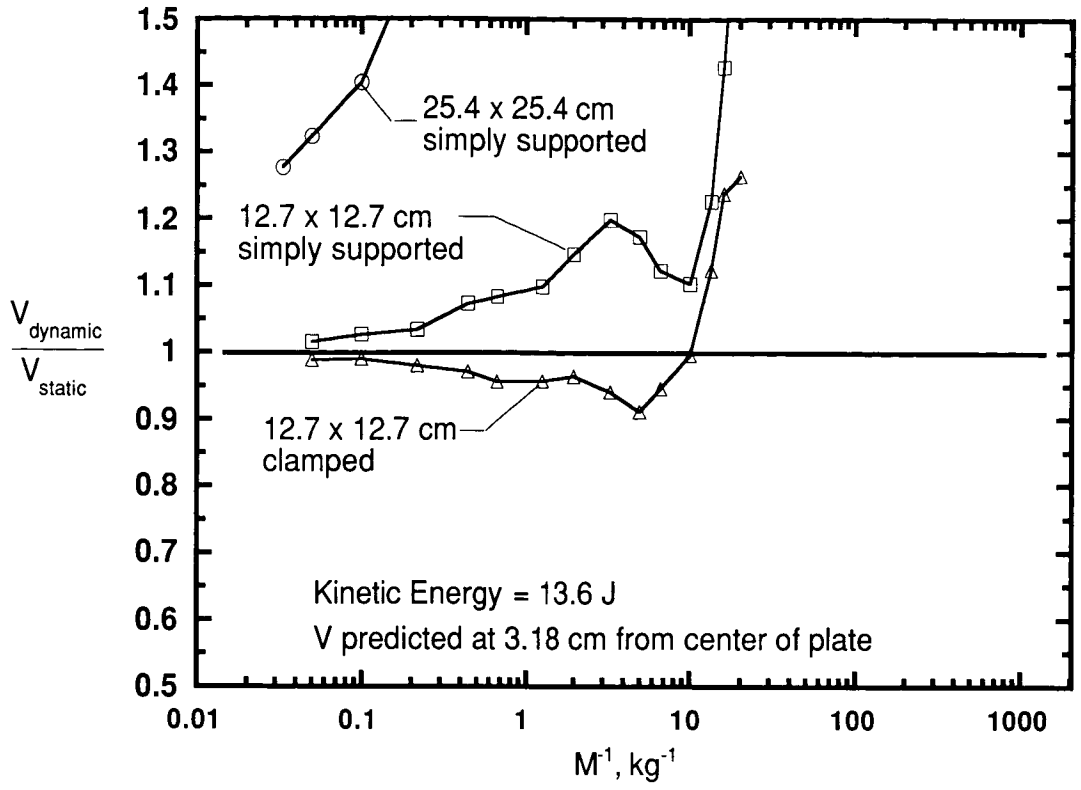

Figure 11. Normalized shear force versus M^{-1} for impacts of plates of various sizes and boundary conditions.

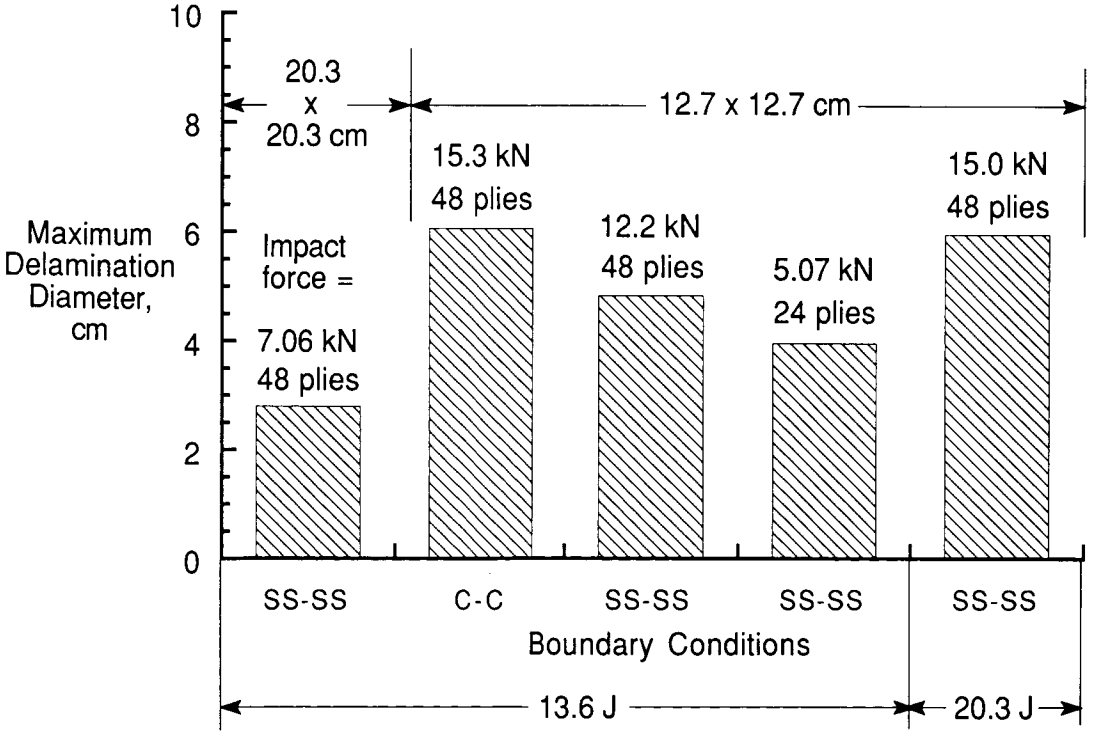

Figure 12. Predicted delamination diameters for two kinetic energies, two plate sizes, two thicknesses, and for clamped and simply-supported edges.

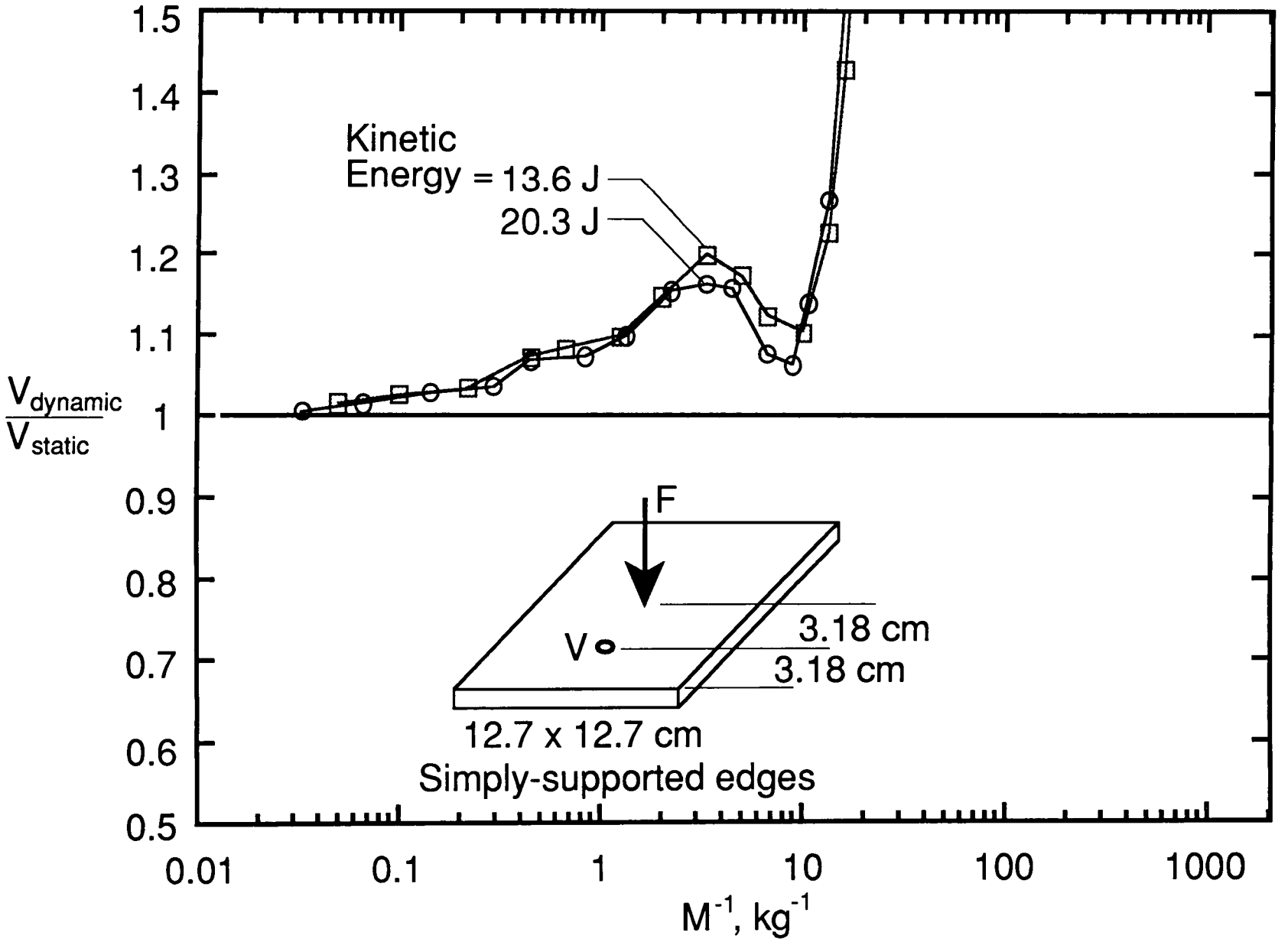

Figure 10. Normalized shear force versus m^{-1} for an impact with a kinetic energy of 13.6 and 20.3 J.